PHYSICAL REVIEW B VOLUME 21, NUMBER 8 15 APRIL 1980

Similarity of (Ga, Al, As) alloys and ultrathin heterostructures: Electronic properties from the empirical pseudopotential method

Wanda Andreoni*
Laboratoire de Physique Appliquée, EPF-Lausanne, Switzerland

R. Car
Laboratoire de Physique Expérimentale, EPF-Lausanne, Switzerland
(Received 10 October 1979)

The energy-band structures of $(GaAs)_n(AlAs)_m$ heterostructures with $2 \leq n + m \leq 8$ and of the corresponding virtual-crystal alloys are calculated with the empirical pseudopotential method. Our results indicate that cation order effects do not play a significant role for these heterostructures and can be handled in perturbation theory. Our picture is in agreement with all the available experimental data. The use for heterostructure calculations of empirical pseudopotentials derived from a fit to the band structures of the pure GaAs and AlAs compounds is critically discussed.

I. INTRODUCTION

GaAs-$Ga_{1-x}Al_xAs$ multilayer heterostructures (HS's) with ranging layer thickness have recently been obtained by molecular beam epitaxy.[1] These HS's are characterized by microscopic potential fluctuations which affect their electronic energy levels depending on the particular repetition lattice constant. When the layer thickness is in the range from a few tens to a few hundreds of Å the HS's show characteristic one-dimensional periodical effects usually referred to as the superlattice regime.[1]

The situation is more intricate for HS's having smaller layer thicknesses, of the order of few GaAs lattice constants. In this case the effects of layering cannot be modeled by simple one-dimensional potential wells, and a full three-dimensional calculation of the energy-band structure is required. A question naturally arises: Are these HS's to be considered as new materials or instead their electronic properties are similar to those of the random alloys with the same composition?

Experimental investigations have been reported for various $(GaAs)_n$-$(AlAs)_m$ HS's with $(n+m)$ ranging from 2 to 10. They include measurements of luminescence,[2,3] optical absorption,[2,4] two-photon absorption,[5] and also Raman and infrared spectra.[6] All these measurements indicate that within differences of the order of ~0.1 eV, the energy levels of ultrathin multilayer HS's are practically indistinguishable from those of the corresponding random alloys. This means that the transition to the superlattice regime, which is controlled by the degree of order of the cation sublattice, takes place rather slowly with increasing layer thickness.

This behavior can qualitatively be understood on the basis of the strong similarity of the two isovalent cations Al and Ga. However, it has not been reproduced by two recent theoretical approaches, one[7-9] based on the empirical pseudopotential method (EPM) and the other[10-12] on the empirical tight-binding method (ETBM). Though quantitative discrepancies exist between the results of these two calculations, they both predict a substantially more rapid transition to the superlattice regime. Particularly interesting in this respect is the pseudopotential calculation of Caruthers and Lin-Chung (CL) which is applied to both alloys and HS's. It predicts significant changes of the electronic properties on passing from the alloy to the HS of the same composition, even in the case of the monolayer HS ($n=m=1$), where a shrinkage of the fundamental gap ranging from 0.3 to 0.5 eV is predicted. This result is quite surprising. Indeed changes of this order of magnitude exist between a typical chalcopyrite compound $A^{II}B^{IV}C_2^V$ (e.g., $ZnGeAs_2$) and its III–V (e.g., GaAs) analog whose properties are expected to differ more, in view of the nonsimilarity of the nonisovalent cations Zn and Ge.

The conflict between experimental data and physical intuition on one side and theoretical predictions on the other side raises a rather puzzling point. In particular, this makes it questionable the use for heterostructure calculations of EPM and ETBM, both adjusted to reproduce the band structures of the pure compounds GaAs and AlAs.

In two previous communications[13,14] we have already shown that with a different and more realistic choice of the pseudopotential difference $\Delta V(r)$ between Ga and Al, the EPM gives results in reasonable agreement with experimental data and provides a more physical picture of the ef-

fects of cation order for HS's with low values of $n=m$.

In this paper we report in more detail our previous calculations and extend them to HS's with larger layer thicknesses and different compositions. We discuss in detail the empirical pseudopotential ΔV responsible in our calculation for cation order effects and compare it with the results of a recent self-consistent pseudopotential calculation on the $n=m=9$ (110) HS (Ref. 15) by Pickett, Louie, and Cohen (PLC). Detailed criticisms and comments on the previous EPM and ETBM calculations are also included.

In Sec. II we describe the crystal structures of $(GaAs)_n$-$(AlAs)_m$ HS's with any (n,m). In Sec. III, after a brief presentation of our method (Sec. III A) we discuss our choice of the pseudopotential ΔV (Sec. III B). Our results for the energy-band structures of various HS's are reported in Sec. IV and compared to experimental data. The final section (Sec. V) is devoted to our conclusions.

II. CRYSTAL STRUCTURE

Both GaAs and AlAs have the zinc-blende structure. Their lattice constants are nearly equal, being $a=5.64$ Å for GaAs and $a=5.63$ Å for AlAs. Owing to the quite perfect matching of the lattice constants, GaAs-AlAs compound systems exhibit very small differences between GaAs and AlAs bond lengths. This suggests that, at least in a first-order approach, one can neglect lattice distortion effects and assume that the atomic positions of the anion and the cation sublattices remain unchanged on going from pure to compound systems. However, compound systems with the same average composition can differ, depending on the particular ordering of the cation sublattice.

When cations are randomly distributed, the resulting system is the homogeneous alloy $Ga_{1-x}Al_xAs$ which can be treated, in a first-order approximation, within the so-called virtual-crystal approximation (VCA). In this approximation the randomly fluctuating cation potential is replaced by a compositionally weighted cation potential and therefore the VC alloys have the same zinc-blende structure as the constituent crystals.

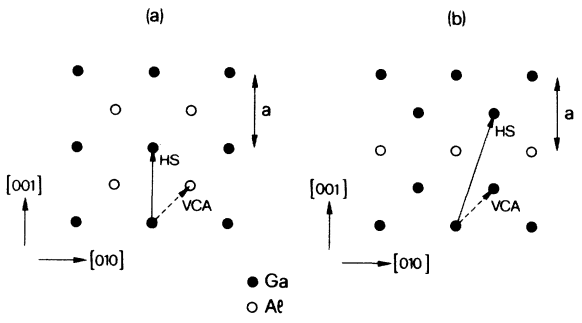

FIG. 1. Cation sublattice on the (100) plane for the (1,1) HS (a) and the (2,1) HS (b). Solid arrow is the HS basic vector; broken arrow, the basic vector of the zinc-blende structure.

TABLE I. Primitive vectors of the direct and of the reciprocal lattice for both D_{2d}^{1} HS's and D_{2d}^{11} HS's. The units are $\frac{1}{2}a$ and $2\pi/a$ for direct and reciprocal lattice vectors, respectively. The reference frame is that of the zinc-blende lattice.

Type of heterostructure	Direct lattice vectors	Reciprocal lattice vectors
even $n+m$	[1, 1, 0]	[1, 1, 0]
(D_{2d}^{1})	[$\bar{1}$, 1, 0]	[$\bar{1}$, 1, 0]
	[0, 0, $n+m$]	[0, 0, $2/(n+m)$]
odd $n=m$	[1, 1, 0]	[1, 1, $1/(n+m)$]
(D_{2d}^{11})	[$\bar{1}$, 1, 0]	[$\bar{1}$, 1, $1/(n+m)$]
	[0, 1, $n+m$]	[0, 0, $2/(n+m)$]

When cations are ordered, so that n GaAs layers are followed repeatedly by m AlAs layers, the system is the $(GaAs)_n$-$(AlAs)_m$ heterostructure and it does not have the zinc-blende structure. In fact some lattice vectors of the face-centered-cubic lattice are not lattice vectors of the heterostructure. This is illustrated in Fig. 1, which represents a cross section of the cation sublattice in the (100) plane for the HS's with $(n+m)=2$ [Fig. 1(a)] and $(n+m)=3$ [Fig. 2(a)]. In each case we show the primitive vectors of the HS and of the VC alloy, with a nonzero component along the [001] direction, which is the direction in which the layer planes are stacked. We notice that for even $(n+m)$, the primitive vector is always parallel to the [001] direction, whereas for odd $(n+m)$, the primitive vector has also a component along the [010] direction. In Table I, we report the basic vectors of the direct and reciprocal lattices for both kinds of HS's.

HS's with even $(n+m)$ have the simple tetragonal structure with spatial symmetry D_{2d}^{1}, while HS's with odd $(n+m)$ have the body-centered-tetragonal structure with spatial symmetry D_{2d}^{11}. In both cases

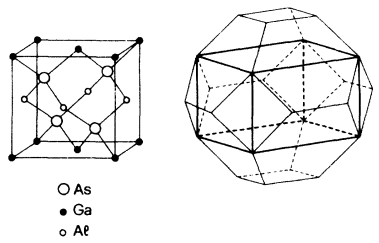

FIG. 2. Direct lattice (left) and Brillouin zone (right) of the (1,1) monolayer HS. The simple tetragonal Brillouin zone of the monolayer is drawn inside the zinc-blende Brillouin zone of the VC alloy.

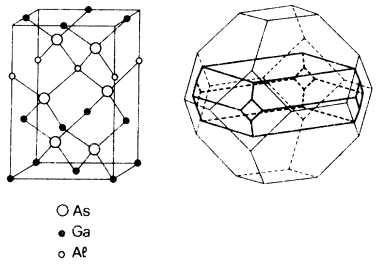

FIG. 3. Direct lattice (left) and Brillouin zone (right) of the (2,1) multilayer HS. The body-centered-tetragonal Brillouin zone of the HS is drawn inside the zinc-blende Brillouin zone of the VC alloy.

the volume of the unit cell is $(n+m)$ times the volume of the unit cell of the zinc-blende structure which results when all the cations are of the same type, as is the case for the corresponding VC alloy. As a consequence the Brillouin zone (BZ) of a $(n+m)$ HS can be obtained by folding $(n+m)$ times the BZ of the corresponding VC alloy. This is illustrated in Fig. 2 for the $(n+m)=2$ and in Fig. 3 for the $(n+m)=3$ HS's.

III. PSEUDOPOTENTIAL APPROACH

A. Outline of the method

We write the potential V_{HS} seen by an electron in the (n,m) HS as

$$V_{\mathrm{HS}}^{(n,m)}(\vec{r}) = V_{\mathrm{ZB}}^{(n,m)}(\vec{r}) + V_{\mathrm{TG}}^{(n,m)}(\vec{r}), \tag{1}$$

i.e., decomposed in its zinc-blende component V_{ZB} which is the potential of the VC alloy $Ga_{1-x}Al_xAs$ of corresponding composition $x=m/(n+m)$,

$$V_{\mathrm{ZB}}^{(n,m)}(\vec{r}) = (1-x)\,V_{\mathrm{GaAs}}(\vec{r}) + x\,V_{\mathrm{AlAs}}(\vec{r}), \tag{2a}$$

and its tetragonal component V_{TG}, which describes cation order and is expressed in terms of the difference ΔV of the two cation potentials

$$V_{\mathrm{TG}}^{(n,m)}(\vec{r}) = \sum_i a_i \Delta V(\vec{r}-\vec{R}_i),$$

$$a_i = \begin{cases} +x, & \text{if } i=\mathrm{Ga} \\ -(1-x), & \text{if } i=\mathrm{Al} \end{cases}, \tag{2b}$$

$$\Delta V(\vec{r}) = V_{\mathrm{GA}}(\vec{r}) - V_{\mathrm{Al}}(\vec{r}).$$

The above expressions allow us to compare directly the HS's to the corresponding VC alloys and show that the difference between the two band structures on the strength of ΔV with respect to V_{ZB}.

We calculate the energy bands of the two systems within the framework of pseudopotential theory, and use empirical pseudopotentials for (2a) and (2b).

First, we determine eigenvalues and eigenfunctions of the alloy Hamiltonian,

$$H_{\mathrm{ZB}}^{(n,m)} = T + V_{\mathrm{ZB}}^{(n,m)}, \tag{3}$$

where T is the kinetic-energy operator and V_{ZB} is defined in (2a). We diagonalize (3) at Γ with 89 plane waves as basis functions, and use the $\vec{k}\cdot\vec{p}$ method[16] for any $\vec{k}$ throughout the BZ. A 15×15 $\vec{k}\cdot\vec{p}$ matrix suffices to give good convergence in the first $\nu\approx10$ energy bands which span an energy range of ~24 eV.

Second, we use the alloy eigenfunctions as a basis set to diagonalize the heterostructure Hamiltonian:

$$H_{\mathrm{HS}}^{(n,m)} = H_{\mathrm{ZB}}^{(n,m)} + V_{\mathrm{TG}}^{(n,m)}. \tag{4}$$

$H_{\mathrm{ZB}}^{(n,m)}$ is obviously diagonal in our basis, while $V_{\mathrm{TG}}^{(n,m)}$ has nonzero matrix elements only between alloy states corresponding to wave vectors $\vec{k}$ and $\vec{k}'$ where $\vec{k}-\vec{k}'$ is a reciprocal lattice vector of the (n,m) HS (see Table I). The energy range we are mainly interested in is that close to the energy gap. In this region, a relatively small number $\nu\approx10$ of alloy bands for each $\vec{k}$ suffices to guarantee the convergence of the HS's. The size of the matrix to be diagonalized for a (n,m) HS is $\approx10\times(n+m)$.

In the case of the monolayer HS, we have numerically verified the accuracy of our procedure to determine differences in the band structures of the two systems in the energy range of interest. No significant change is found when we drop the simplification of the $\vec{k}\cdot\vec{p}$ method in the alloy calculation and use a larger number ν of alloy states for the HS.

B. Choice of the pseudopotential

The VC alloy that we use as starting point for the HS problem has already been studied and fully discussed by Baldereschi *et al.*[17] In particular, they have shown that

(a) the VCA (2a) is appropriate to study the alloy $Ga_{1-x}Al_xAs$ and

(b) their choice of the pseudopotential V_{ZB} is able to reproduce sufficiently well the experimental results over the whole compositional range $(0\le x\le1)$.

In fact, to further investigate the validity of (a), they have estimated the effect of both compositional and positional disorder on the band structure of the VC alloy and showed that disorder produces small effects. They concluded that, since the disorder mainly occurs in the cation sublattice, it cannot have but small effects due to the similarity of the two cations (the electronegativity difference is $\Delta X_{\mathrm{Ga-Al}}=0.06$ according to Phillips[18]).

TABLE II. Comparison of the symmetric and antisymmetric pseudopotential form factors used in recent calculations of GaAs and AlAs. The units are Rydberg and the normalization volume is the atomic volume.

	GaAs			AlAs		
	This work and Ref. 17	CL[a]	PLC[b]	This work and Ref. 16	CL[a]	PLC[b]
V_3^S	−0.2290	−0.2408	−0.2129	−0.2200	−0.2600	−0.2583
V_3^A	0.0700	0.0592	0.1007	0.0720	0.0400	0.0553
V_4^A	0.0600	0.0410	0.0729	0.0625	0.0420	0.0387
V_8^S	0.0123	0.0102	0.0273	0.0260	0.0456	0.0144
V_{11}^S	0.0600	0.0731	0.0477	0.0700	0.0710	0.0425
V_{11}^A	0.0100	0.0231	0.0084	−0.0075	0.0210	0.0032
V_{12}^A	0.0	0.0120	0.0065	0.0	0.0200	0.0031

[a] Reference 8.
[b] Reference 15.

As concerns point (b), a more detailed discussion is needed here, because we use[13,14] thier empirical pseudopotential V_{ZB} not only to recalculate the alloy through (1), but also to derive the individual screened ionic pseudopotentials in V_{TG} (2b). The EPM[19] requires the knowledge of the values of the Fourier transform $V_{ZB}(G)$'s only at a few specific reciprocal lattice vectors of the zinc-blende structure. The values of $V_{ZB}(G)$'s are not unique and depend on the special choices made in the fitting procedure, i.e.,

(1) the experimental data to be fitted,
(2) the cutoff value $G_0[V_{ZB}(G) = 0$ for $G \geq G_0]$,
(3) the number of plane waves used as basis set.

In Table II, we quote three different sets of empirical pseudopotentials for GaAs and AlAs used in two recent calculations of the alloy $Ga_{1-x}Al_xAs$[8,17] and to construct the starting potential in a self-consistent calculation of the (9, 9) (110) HS.[15] In spite of the differences they all reproduce the gross features of the band structures of the pure compounds within the uncertainties of the experimental data and within the typical accuracy of EPM calculations based on local pseudopotentials (~0.1 eV).

From the three sets of pseudopotentials quoted in Table II we can construct three different sets of $V_{ZB}(G)$'s through the VCA (2a). Once the values of $V_{ZB}(G)$'s are adjusted to the system $Ga_{1-x}Al_xAs$, still a large arbitrariness is left in the choice of the individual atomic form factors and in particular of the values $\Delta V(G)$'s which are needed for the calculation of the HS's. Moreover, in order to obtain the values of $\Delta V(q)$ at the additional reciprocal lattice vectors of the tetragonal structure (Table I), an extrapolation is required. Throughout this procedure, the discrepancies between the three choices of $V_{ZB}(G)$'s, become of critical importance.

In Table III we quote three different sets of values of the difference $\Delta V(q)$ of the cation pseudopotentials: the one corresponding to the first choice of pseudopotentials in Table II and used in the present calculation, the one corresponding to the second choice of pseudopotentials in Table II and used by CL[7-9] in their calculation of the HS's, and finally, the one corresponding to the last choice of pseudopotentials in Table III and used by PLC (Ref. 15) in the first iteration of their self-consistent calculation of the (9, 9) HS. The differences are already very large for the values of q which correspond to the reciprocal lattice vectors of the ZB structure. For smaller q values, the results of the three extrapolations are also strikingly different. In particular, our values are at least one order of magnitude smaller than

TABLE III. Atomic pseudopotential difference $\Delta V \equiv V_{Ga} - V_{Al}$ (in eV, normalized to the atomic volume) at some selected reciprocal lattice vectors of the tetragonal structure. The PLC data refer to their starting (i.e., non-self-consistent) atomic form factors.

$G/\frac{2\pi}{a}$	$\Delta V \equiv V_{Ga} - V_{Al}$ This work	CL[a]	PLC[b]
(0, 0, 1)	−0.028	0.980	−3.057
(1, 1, 0)	−0.059	1.088	−1.688
(1, 1, 1)	−0.155	0.522	−1.234
(2, 0, 0)	−0.193	−0.027	−0.931
(2, 2, 0)	−0.080	−0.963	−0.352
(3, 1, 1)	0.098	0.060	−0.141
(2, 2, 2)	0.137	−0.218	−0.091

[a] Reference 8.
[b] Reference 15.

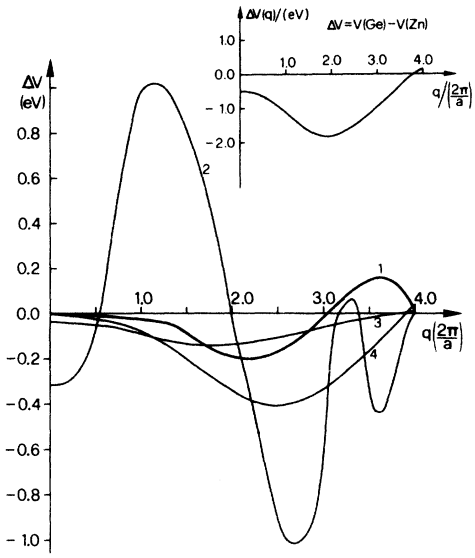

FIG. 4. Screened Ga-Al pseudopotential difference ΔV in momentum space. ΔV is normalized to the atomic volume. Curve 1, present work (from Ref. 17); curve 2, Caruthers and Lin-Chung (Ref. 8); curve 4, ionic core Ga-Al pseudopotential difference used by Pickett, Louie, and Cohen (Ref. 15), screened with the Penn dielectric function (Ref. 21) of GaAs; curve 3 = ΔV from the Animalu-Heine model (Ref. 20) screened with the Penn (Ref. 21) dielectric function of GaAs. The insert gives the core Ge – Zn pseudopotential difference calculated from the Animalu-Heine model (Ref. 20) screened with Penn dielectric function (Ref. 21) of GaAs.

the other two.

In Fig. 4, our $\Delta V(q)$ is compared to $\Delta V_{CL}(q)$ (curve 2), in the whole range of q. The shape and smaller values of our $\Delta V(q)$ are supported by several reasons:

(i) Since Ga and Al are isovalent, ΔV represents only core differences which are not much relevant to their chemical properties (Phillip's electronegativities,[18] proper to ions in tetrahedral environment are 1.13 and 1.18, respectively) and in real space are confined to a small region near the nucleus.

(ii) As shown in Fig. 4, our $\Delta V(q)$ quantitatively agrees with the one (curve 3) derived by subtracting the Ga and Al model potentials of Animalu-Heine[20] (AH) and screening the difference with Penn dielectric function of GaAs (Ref. 21); Animalu-Heine model accounts for the similarity of the atomic energy spectra of Ga and Al.

(iii) In their self-consistent calculation, PLC (Ref. 15) have found that the order of magnitude of their initial atomic form factors (Table III) is not realistic; in fact, e.g., the consistency procedure changes the difference between the average bulk potentials $\Delta\overline{V} = \overline{V}_{AlAs} - \overline{V}_{GaAs}$ from the initial value of 1.70 eV to the final value of −0.05 eV.

It is well known that in a self-consistent calculation, the choice of the starting potential is not relevant to the final results, which only depend on the choice of the ion-core potentials. PLC used model ion-core pseudopotentials derived from those of Heine–Abarenkov[22] (see note in Ref. 23). The self-consistency constraint, which accounts for the screening of the core potentials due to the valence electrons in the crystal, has the effect of weakening the difference between the bare ionic pseudopotentials. We expect that their final ΔV does not suffer significantly from the one obtained by screening the difference of their bare Ga and Al ionic pseudopotentials with Penn dielectric model: The result of this procedure is shown in Fig. 4 (curve 4) and its order of magnitude definitely confirms our choice. We point out that the values of this final ΔV differ from the starting ones (Table III, 3rd column) by one order of magnitude. Therefore, after comparing the work of PLC to that of CL, one can reasonably expect that the values of ΔV used by CL in a non-self-consistent calculation of HS's[7-9] would be changed significantly by the self-consistency requirement. We also notice that the results of PLC indicate that only a negligible redistribution of charge, particularly of the bonding charge, occurs at the interface from GaAs to AlAs and this is again a consequence of the strong similarity of the two cations [see (i)].

However, some criticism which is common to all previous calculations of alloys and HS's, can

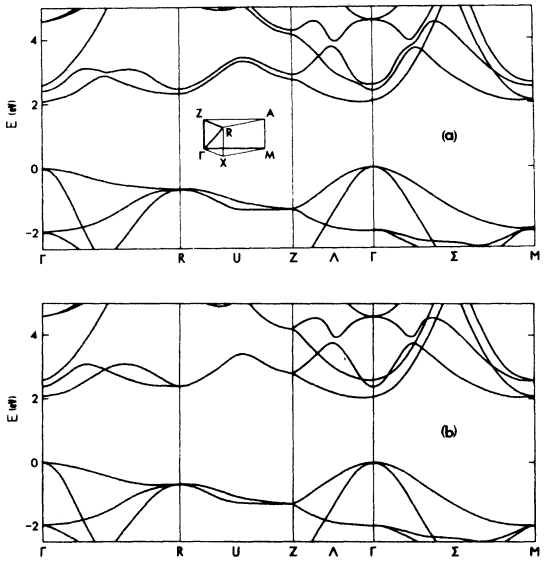

FIG. 5. Band structure of $(GaAs)_1 - (AlAs)_1$ (a) and $Ga_{0.5}Al_{0.5}As$ (b). The insert in (a) gives the irreducible Brillouin zone of the simple tetragonal structure.

also be made. All calculations in fact, neglect the nonlocality of the pseudopotentials and the spin-orbit interaction. Nonlocality properties of the pseudopotentials might be relevant, particularly for an accurate description of the charge distribution, as shown in the case of GaAs.[24] Nonlocality emphasizes the core difference between Ga and Al, mostly due to the presence of d states in the core of Ga. However, as previously dicussed in (i), whatever description of the core differences cannot qualitatively affect our conclusions on ΔV. Spin-orbit effects show a nonlinear variation with composition in several alloys[25,26] and the validity of the VCA in explaining this behavior is still questionable.[26] Spin-orbit effects, however, should not be relevant to any modification of electronic states near the band edges from the alloys to the HS's; in fact spin orbit coupling is especially important for the valence states which, being anionic, remain essentially unaltered by the cation ordering.

IV. THEORETICAL RESULTS AND COMPARISON WITH EXPERIMENTAL DATA

A. (1,1) heterostructure

The energy bands of the (1, 1) monolayer HS [Fig. 5(a)] are very similar to those of the $Ga_{0.5}Al_{0.5}As$ VC alloy [Fig. 5(b)] folded into the tetragonal BZ. Energy differences are generally of the order of 0.01 eV and they become of the order of 0.1 eV whenever the tetragonal potential V_{TG} couples alloy states which are degenerate either by symmetry (i.e., all the states lying on the external faces of the irreducible tetragonal BZ as illustrated along U, in Fig. 5) or accidentally [e.g., all the band crossings appearing in Fig. 5(b) and not in Fig. 5(a)].

According to our previous discussion in Sec. III B, the additional potential V_{TG} is only a weak perturbation on V_{ZB}, since the average strength of ΔV is only 0.1 eV. We have verified that perturbation theory can be applied to the alloy bands [Fig. 5(b)] and gives, at the lowest nonzero order, the correct splittings in the HS. In fact the tetragonal perturbation acts in first order when it couples degenerate alloy states, and in second order it couples alloy states which are generally separated by ~1 eV or more. Both the small V_{TG} and the large energy denominators contribute to the validity of the perturbative argument.

The splitting ΔE_v of the topmost valence-band state Γ_{15v} and the lower singly degenerate Γ_{4v} amounts only to ~2 meV. However our nonrelativistic calculation should be corrected here by the effect of the spin-orbit interaction which, in the absence of the tetragonal perturbation, splits the Γ_{15v} state into the two levels Γ_{8v} and Γ_{7v}. The spin-orbit splitting Δ_{so} is larger than ΔE_v [Δ'_{so} = 0.34 eV for GaAs and Δ''_{so} = 0.29 eV for AlAs (Ref. 27)] and cannot be neglected. When both the spin-orbit interaction and the tetragonal perturbation are taken together, the Γ_{15v} state splits into the three levels Γ_{6v}, Γ^{+}_{7v}, and Γ^{-}_{7v}.

The relative position of the triplet levels of the HS with respect to the doublet levels (Γ_{8v} and Γ_{7v}) of the alloy is determined by V_{TG} as well as by the tetragonal component V^{so}_{TG} of the spin-orbit potential in the HS Hamiltonian. As already noted for V_{TG}, also V^{so}_{TG} acts as a second-order perturbation on the topmost valence band at Γ in the alloy. The average strength of V^{so}_{TG} is $\Delta'_{so} - \Delta''_{so}$ = 0.05 eV for the levels under consideration and is therefore comparable with the average ΔV. This does not allow us to make any quantitative estimate of the final splitting in the HS. However, a qualitative estimate can be made if we neglect the effect of V^{so}_{TG}. In this case, the energies of the triplet levels of the HS with respect to the initial Γ_{15v} level of the alloy are given by

$$\begin{aligned} E(\Gamma_6) &= +\tfrac{1}{3}\Delta_{so}, \\ E(\Gamma_7^{\pm}) &= E(\Gamma_6) - \tfrac{1}{2}(\Delta_{so} + \Delta E_v) \\ &\quad \pm \tfrac{1}{2}[(\Delta_{so} + \Delta E_v)^2 - \tfrac{8}{3}\Delta_{so}\Delta E_v]^{1/2} \end{aligned} \tag{5}$$

in terms of the spin-orbit splitting Δ_{so} of the alloy doublet and of the tetragonal splitting ΔE_v. Equations 5 constitute the so-called "quasicubic" model of Hopfield[28] and have already been applied to crystals of the wurtzite type[29] and of the chalcopyrite type.[30] Since in our case ΔE_v is much smaller than Δ_{so}, we can further simplify Eqs. (5) by a first-order expansion with respect to ΔE_v, giving

$$\begin{aligned} E(\Gamma_6) &= +\tfrac{1}{3}\Delta_{so}, \\ E(\Gamma^{+}_{7v}) &= E(\Gamma_6) - \tfrac{2}{3}\Delta E_v, \\ E(\Gamma^{-}_{7v}) &= E(\Gamma_6) - \Delta_{so} - \tfrac{1}{3}\Delta E_v. \end{aligned} \tag{6}$$

This description is quite general and applies to any (n, m) HS. A schematic representation of the resulting valence band structure near the Γ point is given in Fig. 6, which shows the different splittings of the state Γ_{15v} of the alloy that occur as a consequence of the spin-orbit and of the crystal-field interaction. We notice that the crystal-field interaction has the effect of pushing downward the heavy-hole band edge with respect to the light-hole band edge. This can be explained by considering that ΔE_v is due to V_{TG} acting in second order and that the interaction of the top of the valence band with the conduction-band states dominates over the interaction with the lower valence-band states, since V_{TG} is mostly localized in the cation

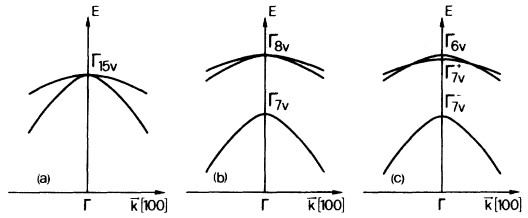

FIG. 6. Schematic representation of the topmost group of valence bands near the point Γ for (a) the VC alloy without the inclusion of spin-orbit interaction, (b) the VC alloy with the inclusion of spin-orbit interaction, and (c) the heterostructure with the inclusion of spin-orbit interaction.

sublattice. The calculated splitting $\frac{2}{3}\Delta E_v \sim 1.3$ meV between the light- and heavy-hole bands, however, should be considered only as an order of magnitude, because its quantitative estimate is very critical as it depends on ΔV to the second order. Also its sign is quite uncertain in view of the neglect of V_{TG}^{so} is our approximation. In any case our calculated splitting for the (1, 1) HS is in order-of-magnitude agreement with the 5.3-meV splitting observed in the (9, 1) HS (Ref. 5) by measuring the two-photon absorption spectrum,[31] where in addition the polarization data indicate that the heavy-hole band edge has the lowest energy. CL (Refs. 7 and 8) obtain instead $\Delta E_v \sim 170$ meV, due to the too large strength of their ΔV, discussed above (Sec. III B). We notice that the self-consistent calculation of PLC (Ref. 15) gives $\Delta E_v \sim 50$ meV in the (9,9) HS where layering effects are expected to be larger.

In Fig. 7, we report the charge density corresponding to the valence state Γ_{4v}. The charge is heavily concentrated on the bonds and has still the

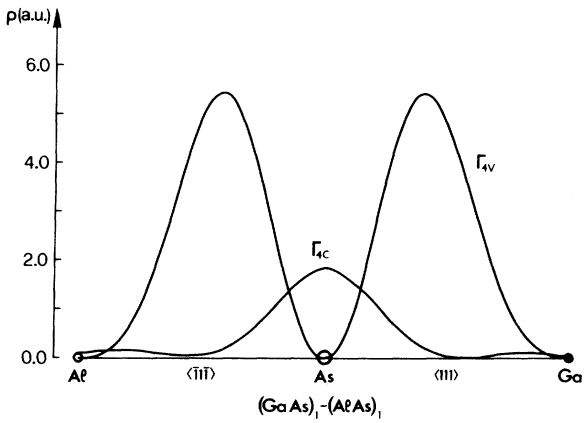

FIG. 7. Charge density corresponding to the states Γ_{4v} (lower state of the topmost group of valence bands at Γ) and Γ_{4c} (lowest conduction state at Γ) for $(GaAs)_1 - (AlAs)_1$ along two bond directions.

character of a VC alloy state since only negligible asymmetry exists between Ga-As and Al-As bonds.

Both the VC alloy and the monolayer are *indirect*, the conduction-band minimum of the monolayer lying on the Λ line (Δ_Z axis in the zinc-blende BZ). The indirect gap $E_{gi} = 2.05$ eV of the monolayer is ~1 meV smaller than the calculated one in the alloy. The experimental value for E_{gi} reported in Ref. 4 is ~2.06 eV. In agreement with experimental evidence,[4] the lowest gap $E_{gd}^{(1)}$ of the HS at Γ ($\Gamma_{5v} \rightarrow \Gamma_{4c}$) is pseudodirect, i.e., the one-photon transitions are weakly allowed, since the final state Γ_{4c} derives from the X point of the zinc-blende BZ and is only slightly modified by V_{TG}. In Fig. 7 the corresponding charge density exhibits only a negligible difference between the values along the two bond directions, in agreement with perturbative arguments. In practice, this allows one to classify still the Bloch states in the monolayer with the momentum of the zinc-blende BZ.

In our calculation, $E_{gd}^{(1)}$ is ~20 meV wider than our indirect gap E_{gi}. Intense optical absorption starts at $E = E_{gd}^{(2)} = 280$ meV above $E_{gd}^{(1)}$, in correspondence to transitions from the Γ_{5v} state to the upper conduction state Γ_{1c}. The ratio of oscillator strengths of the pseudodirect and the direct optical transition at Γ is less than 10^{-3}.

Our results strongly disagree with those of CL (Refs. 7 and 8). According to these authors the VC alloy is indirect whereas the monolayer HS is nearly direct. Moreover, they find both the pseudodirect gap $E_{gd}^{(1)}$ and the direct gap $E_{gd}^{(2)}$ of the monolayer smaller than the indirect gap of the corresponding VC alloy by ~0.5 eV (or ~0.3 eV with modified pseudopotential form factors[8]) and by ~0.2 eV, respectively. Since the experimentally measured gaps[2,4,5] are larger, CL (Ref. 8) interpreted the discrepancy as due to the disorder existing in the samples of the monolayer HS used in the experiments. Disorder effects, however, are unlikely to increase the monolayer gaps by such a large amount. In fact, energy shifts due to disorder in GaAlAs compound materials are expected to be smaller than 0.1 eV, as can be deduced by the observed bowings of the band gaps in the alloys, where, in addition, they act in the opposite sense[32] (i.e., tend to decrease the band gaps).

Comparison of theoretical and experimental results is made more difficult by the presence of compositional and positional disorder both in the HS's and in the alloy samples. Furthermore, it is very difficult to obtain HS and alloy samples with exactly the same composition. All these effects originate some scattering in the experimental data (for instance, the experimental values for the indirect gap of the $Ga_{0.5}Al_{0.5}As$ alloy range from[23] 1.9 to 2.1 eV). However, transmission electron

microscopy[4] and x-ray diffraction[34] confirm that the HS's are substantially more ordered than the corresponding alloys. All these considerations are important when comparing theory and experiment. Our calculation predicts that the onset of both indirect and direct transitions does not significantly change on going from the VC alloy to the monolayer, whereas optical data[4] indicate that both E_{gi} and $E_{gd}^{(2)}$ are wider in the HS, by ~70 and 110 meV, respectively. This discrepancy is reduced if we correct our VC alloy values by the downward bowings observed in the real alloy. It should be noticed, however, that the monolayer and the alloy samples used in Ref. 4, were not of exactly the same composition.

A more conclusive argument in favor of the strong similarity of the monolayer and the alloy is given by very recent experimental data by Miller.[3] In a very accurate experiment he was able to see the variation of the luminescence of a monolayer sample when this was changed into an alloy sample by annealing. His results indicate that the fundamental gap of the alternate monolayer is within 50 meV of the band gap of the alloy.

As a final remark, we point out that also the results of a TB calculation by Schulman and McGill[12] (SM) for the (1,1) monolayer HS give a fundamental gap of 2.16 eV, very close to the alloy gap which is of 2.18 eV according to SM.

B. (n,n) heterostructures

We have seen that the (1,1) HS is very similar to the VC alloy. It is also evident that the (n,n) HS with large n has a gap which tends to that of GaAs. We have therefore calculated the electronic states at the band edges of HS's with $n=m=2,3,4$ in the attempt to determine when cation order starts to play a significant role.[13,14] We did not extend our investigation to HS's with larger n, because this requires the knowledge of the pseudopotential at small q values where a self-consistent calculation is probably necessary.

In Fig. 8 the energy levels at Γ are shown for the different monolayer HS's and compared to the corresponding levels of the alloy $Ga_{0.5}Al_{0.5}As$. The splitting of the top valence bands at Γ remains of the same order as in the monolayer; the shrinkage ΔE_g of the lowest, still pseudodirect gap is also very weak: $\Delta E_g = 4$, 10, and 16 meV for $n=2,3,4$, respectively. This gap decrease is in qualitative agreement with the results of the empirical tight-binding calculations of SM (Refs. 10–12); however, their values are one order of magnitude larger [e.g., $E_g(n=2)-E_g(n=3)\simeq 80$ meV compared to our 6 meV]. As already discussed in Ref. 13, our values are supported by experimental data on ultrathin HS's (Ref. 2) where

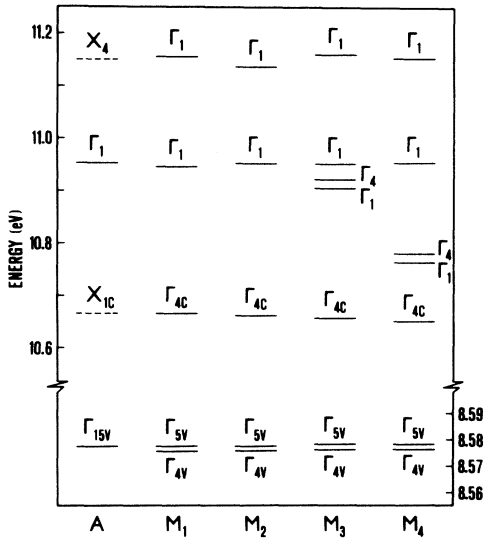

FIG. 8. Calculated energy levels at Γ for $(GaAs)_n$ – $(AlAs)_n$ monolayers (M_n) compared to those at Γ and X of the virtual-crystal alloy (A).

the absorption edge seems to be only weakly dependent on n. The gap $\Gamma_{5v}-\Gamma_{1c}$ shrinks more rapidly for $n\geq 3$, due to the appearance of new lower Γ_1 states which result from Λ states folded into Γ. The progressive folding of the BZ in HS's with $n>4$ will eventually cause the Γ_1 level to cross the Γ_4 level, in qualitative agreement with the results of CL.[9] As n increases, this mechanism appears to be the one responsible for the further narrowing of the lowest gap that eventually merges with the GaAs gap which is direct and ~0.5 eV smaller.

For low n, our results show that the HS's are still indirect and similar to the alloy; the tetragonal potential can still be treated as a weak perturbation acting on the zinc-blende VC alloy. Consequently the electron states at the band edges keep their nature of "alloy states" as in the monolayer.

CL (Ref. 9) show their results only for the three lowest conduction states at Γ for $1\leq n\leq 9$ and discuss the cases $n=3$ and 9. As in the case of the monolayer, all these HS's exhibit substantial differences with the alloy; however the energy variations with increasing n are one order of magnitude smaller than the difference between monolayer and alloy. According to CL the two lowest conduction states are GaAs states and the third is an AlAs state. This would indicate that the transition to the superlattice regime starts to take place quite rapidly. In particular, in the trilayer they already find a charge transfer of $0.2e$ from GaAs layers to AlAs layers through the interface. This disagrees with the results of PLC (Ref. 15)

who obtain a negligible charge transfer of $0.02e$ even in the 9-layer HS.

The ETB calculation of SM (Refs. 10 and 12) gives an even faster shrinkage of the direct band gap for increasing n, due to the lowering of the level at Γ. Their TB parameters were adjusted to fit two independent pseudopotential results[35] for the pure compounds and, in particular, the band gaps. They are not able to reproduce the conduction bands sufficiently well and this is probably the reason why in their calculation the (n,n) HS's are direct for $n \geq 2$.[12] They also find that, already in the bilayer,[10] the band-edge wave functions are almost entirely confined to GaAs layers. It is not easy to understand what gives rise to this behavior. Indeed, it is well known that the TB method, when used as a Slater-Koster[36] interpolation scheme, by assuming nonoverlapping Wannier functions and a limited number of interactions, does not give reliable wave functions in semiconductors, particularly for the conduction states.[37] Comments about the dependence of TB parameters on the fitting procedure can be made, analogous to those made in Sec. III B about the choice of the empirical pseudopotentials. In addition, in the ETBM the wave functions are particularly sensitive to the quality of the fitting itself. On going from a ZB lattice to a superlattice, the ETBM does not present intrinsic difficulties as the EPM does, due to the ignorance of the form factors for small q values. However, one should notice that, due to the progressive folding of the BZ, the quality of the TB fitting for the HS's is guaranteed only if the original one reproduced well the bands inside the original BZ.

We remark that the results of SM (Refs. 10–12) for the HS's with larger number of layers ($n=7$ or 10) do not agree with those of PLC.[15] In fact SM describe the states at the band edges as superlattice states confined to GaAs potential wells, while PLC find that the (9,9) HS still belongs to an intermediate regime of interacting potential wells.

C. (n,m) heterostructures with $n \neq m$

We have calculated a few HS's with $n \neq m$ and with compositions $x=0.33$ $(n+m=3$ and 6), $x=0.25$ $(n+m=4)$, $x=0.75$ $(n+m=4)$, and $x=0.67$ $(n+m=3)$.

Our results show again a strong similarity between HS's and VC alloys. The energy differences are of the same order as for the HS's with $x=0.5$ and the band-edge wave functions do not show any definite preferential confinement, in contrast with the results of SM,[10-12] who obtain band-edge wave functions heavily confined to GaAs layers in the whole range of the composition considered $(0.25 \leq x \leq 0.67)$. Furthermore, the HS's are direct or indirect according to the direct or indirect character of the corresponding alloys.

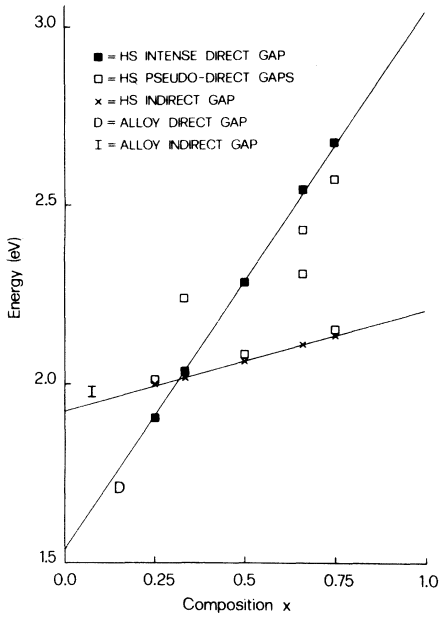

FIG. 9. Variation with the composition x of the lowest direct gaps and of the indirect gap for the HS's and the VC alloys.

In Fig. 9, we report the values of the lowest direct gaps and of the indirect gap for the HS's and for the VC alloys.[17] It should be noticed that all our results have been obtained with a nonrelativistic EPM calculation and therefore spin-orbit corrections should be added to the values of Fig. 9 before comparing them with the experimental data. However, as already remarked in Sec. III B, we do not expect that spin-orbit effects significantly change on passing from the HS's to the alloys.

Both direct and indirect gaps of the various HS's scale almost linearly with composition, thus reproducing the behavior of those of the VC alloys. This is a consequence of the weakness of our tetragonal potential V_{TG} with respect to V_{ZB} [Eq. (1)]. In fact, V_{TG} [Eq. (2b)], when acting as a second-order perturbation on the energy levels, would introduce a nonlinear dependence with composition.

The available experimental data are very few[4] and cover only a limited portion of the x range. The gaps of the HS's have been measured for $x \approx 0.12$, 0.35, 0.50, and 0.60 and compared to the alloy gaps obtained from interpolation formulas.[38] In both cases, they show a quite linear variation with composition, confirming our theoretical prediction. Again, the experimental data seem to indicate that the HS gaps are wider than those of the corresponding alloys by ~60–70 meV. The comments already made in Sec. IV A for the monolayer

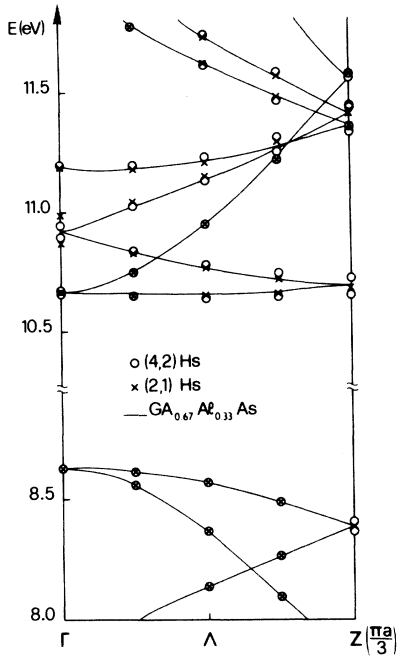

FIG. 10. Energy bands of $Ga_{0.67}Al_{0.33}As$, of $(GaAs)_2-(AlAs)_1$, and of $(GaAs)_4-(AlAs)_2$ along the Λ direction of the body-centered-tetragonal Brillouin zone.

retain their validity for the (n,m) HS's.

As shown in Fig. 9 the direct and indirect gaps cross at $x \equiv x_0 = 0.34$. The lowest direct gap of the HS corresponds to the direct alloy gap for $x \leq x_0$ and becomes pseudodirect for $x > x_0$, in correspondence to the folding of a $\vec{k}$ point in the Λ direction (Δ in the zinc-blende BZ) of the alloy into Γ.

We have studied the effect of increasing the number of layers for $x = 0.33$. For $n+m = 6$ we find that the folding of the X point causes the pseudodirect gap to cross the direct gap. A more detailed comparison between the electronic states of the $x = 0.33$ VC alloy and those of the (2,1) and the (4,2) HS's is given in Fig. 10, where the energy bands of the three systems are reported along the Λ direction. Layering effects are not yet evident, even if the first conduction band seems to show the tendency to separate into a miniband on going from the (2,1) to the (4,2) HS.

V. CONCLUSIONS

The calculations presented in this paper show that the electronic properties of $(GaAs)_n-(AlAs)_m$ HS's with $n+m \leq 8$ are very similar to those of the corresponding alloys $Ga_{1-x}As_xAs$. This seems to limit the importance of these ultrathin HS's for practical applications.

Our results agree with all available experimental data, but disagree with the results of previous calculations based on the EPM (Refs. 7–9) and on the ETBM (Refs. 10–12) which both indicated a rather rapid transition from the alloy to the superlattice regime. In Secs. III B and IV we have fully explained the reasons of these discrepancies. An important consequence of our investigation is that empirical calculations which fit reasonably well the energy bands of GaAs and AlAs do not necessarily give equally good results for the HS's.

It is interesting to compare our results for the monolayer (1,1) HS to the well-established data[39] for $A^{II}B^{IV}C_2^V$ chalcopyrite compounds, in particular those where atoms A and B belong to the same row of the periodic table, so that crystallographic distortions are negligible. The chalcopyrite (e.g., $ZnGeAs_2$) can be considered as an HS and the zinc-blende binary analog (e.g., GaAs) plays the role of the alloy. By analogy with the formulation presented in this paper, the chalcopyrite crystal potential can be written as the sum of the potential of the zinc-blende binary analog (V'_{ZB}) and of a tetragonal component (V'_{TG}). In this case, however, the two cations (Zn and Ge) are not isovalent and their potential difference $\Delta V'$ is stronger and long range in real space. In the insert of Fig. 4 we report the q-space dependence of the screened-core pseudopotential difference $\Delta V'$ (Zn-Ge) calculated from the Animalu-Heine model.[20] $\Delta V'$ is larger than ΔV (Ga-Al) by an order of magnitude and therefore, according to our perturbative argument, we expect the effects on the energy bands to be ~100 times larger. Experimental data[39] show that the fundamental gaps of chalcopyrites differ from those of the III-V analog compounds by ~0.3 eV at most. This would imply a fundamental-gap shrinkage of ~3 meV on passing from $Ga_{0.5}Al_{0.5}As$ to the (1,1) HS which further confirms our results. The analogy with the chalcopyrite compounds indicates that cation order will produce effects of the order of 0.1 eV in the energy bands of nonisovalent HS's like Ge_n-$(GaAs)_n$ for low n.

We expect therefore that the similarity found in the present work between ultrathin HS's and the corresponding $Ga_{1-x}Al_xAs$ alloys will generally apply to superlattices made of a small number of alternating isovalent atoms and also to nonisovalent systems though the energy differences will be somewhat larger in this case.

ACKNOWLEDGMENTS

We are grateful to Dr. A. Baldereschi for suggesting this problem and for helpful discussions. We wish to thank Dr. R. C. Miller for sending us unpublished data on the monolayer heterostructure. Thanks are also due to Dr. S. Louie and Dr. W. Pickett for useful discussions and to Dr. E. Tosatti for a critical reading of the manuscript.

*Present address: Bell Laboratories, Murray Hill, New Jersey 07974.
[1]G. A. Sai-Halasz, Inst. Phys. Conf. Ser. 43, 21 (1979), and references therein.
[2]A. C. Gossard, P. M. Petroff, W. Wiegmann, R. Dingle, and A. Savage, Appl. Phys. Lett. 29, 323 (1976).
[3]R. C. Miller, private communication. The new results (see Sec. IV A) modify the conclusions about a monolayer gap ~0.2 eV smaller than that of $Ga_{0.5}Al_{0.5}As$ alloy, reported in R. C. Miller, D. A. Kleinmann, and A. C. Gossard, Inst. Phys. Conf. Ser. 43, 1043 (1979).
[4]J. P. van der Ziel and A. C. Gossard, J. Appl. Phys. 48, 3018 (1977).
[5]J. P. van der Ziel and A. C. Gossard, Phys. Rev. B 17, 765 (1978).
[6]A. S. Barker, Jr., J. L. Merz, and A. C. Gossard, Phys. Rev. B 17, 3181 (1978).
[7]E. Caruthers and P. J. Lin-Chung, Phys. Rev. Lett. 38, 1543 (1977).
[8]E. Caruthers and P. J. Lin-Chung, Phys. Rev. B 17, 2705 (1978).
[9]E. Caruthers and P. J. Lin-Chung, J. Vac. Sci. Technol. 15, (1978).
[10]J. N. Schulmann and T. C. McGill, Phys. Rev. Lett. 39, 1680 (1977).
[11]J. N. Schulmann and T. C. McGill, J. Vac. Sci. Technol. 15, 1456 (1978).
[12]J. N. Schulmann and T. C. McGill, Phys. Rev. B 19, 6341 (1979).
[13]W. Andreoni, A. Baldereschi, and R. Car, Solid State Commun. 27, 821 (1978).
[14]W. Andreoni, R. Car, and A. Baldereschi, Inst. Phys. Conf. Ser. 43, 733 (1979).
[15]W. E. Pickett, S. G. Louie, and M. L. Cohen, Phys. Rev. B 17, 815 (1978).
[16]W. Brinkman and B. Goodman, Phys. Rev. 149, 597 (1966).
[17]A. Baldereschi, E. Hess, K. Maschke, H. Neumann, K. R. Schulze, and K. Unger, J. Phys. C 10, 4709 (1977).
[18]J. C. Phillips, *Bands and Bonds in Semiconductors* (Academic, New York, 1973), p. 54.
[19]M. L. Cohen and V. Heine, in *Solid State Physics*, edited by Seitz and Turnbull (Academic, New York, 1970), Vol. 24, p. 37.
[20]A. O. E. Animalu and V. Heine, Phil. Mag. 12, 1249 (1965).
[21]D. R. Penn, Phys. Rev. 128, 2093 (1962).
[22]I. V. Abarenkov and V. Heine, Phil. Mag. 12, 529 (1965).
[23]The reduction of energy- and angular-momentum-dependent model pseudopotentials (such as Heine-Abarenkov and Animalu-Heine models) to a fully local form contains some ambiguity. One usually extrapolates the nonlocal models to a common mean energy value such as the Fermi energy, and averages out the l dependence. Especially due to the ambiguity in the choice of the mean energy, quantitative differences can exist between different local pseudopotentials derived in this way. See the discussion in J. R. Chelikowsky and M. L. Cohen, Phys. Rev. 10, 5095 (1974).
[24]K. C. Pandey and J. C. Phillips, Phys. Rev. B 9, 1552 (1974); J. R. Chelikowsky and M. L. Cohen, *ibid.* B 14, 556 (1976).
[25]O. Berolo and J. C. Woolley, in *Proceedings of the Eleventh International Conference on the Physics of Semiconductors*, edited by M. Miasek (Elsevier PWN—Polish Scientific, Warsaw, 1972), p. 1420; J. van Vechten, E. Berolo, and J. C. Woolley, Phys. Rev. Lett. 29, 1400 (1972).
[26]D. J. Chadi, Phys. Rev. B 16, 790 (1977).
[27]Reference 18, Table 7.3.
[28]J. J. Hopfield, J. Phys. Chem. Sol. 15, 97 (1960).
[29]B. Segall and D. T. F. Marple, in *The Physics and Chemistry of II–VI Semiconductors*, edited by M. Auer and J. S. Prener (North-Holland, Amsterdam, 1967).
[30]J. L. Shay, E. Buhler, and J. H. Wernick, Phys. Rev. B 3, 2004 (1971).
[31]The measured splitting is also due to strain and to exchange splitting which together contribute ~1 meV of the observed splitting (Ref. 5).
[32]For a discussion of disorder effects in $Ga_{1-x}Al_xAs$, see Ref. 17.
[33]For a complete reference on these data see Ref. 17.
[34]P. D. Dernier, D. E. Moncton, D. B. McWhan, A. C. Gossard, and W. Wiegmann, Bull. Am. Phys. Soc. 22, 293 (1977).
[35]J. R. Chelikowsky and M. L. Cohen in Ref. 22 (GaAs); H. Hess, I. Topol, K. R. Schulze, H. H. Neumann, and K. Unger, Phys. Status Solidi (B) 55, 187 (1973) (AlAs).
[36]J. C. Slater and G. F. Koster, Phys. Rev. 94, 1498 (1954).
[37]See the discussion in D. J. Chadi, Phys. Rev. B 16, 3572 (1977).
[38]M. A. Afromowitz, Solid State Commun. 15, 59 (1974); H. C. Casey, Jr. and M. B. Panish, J. Appl. Phys. 40, 4970 (1959).
[39]J. L. Shay and J. H. Wernick, *Ternary Chalcopyrite Semiconductors* (Pergamon, Oxford, 1975), Chap. III, p. 85, in particular.